

# EVALUATION OF LICHTENECKER'S MIXING MODEL FOR PREDICTING EFFECTIVE PERMITTIVITY OF SOILS AT 50 MHz

T. P. Leão, E. Perfect, J. S. Tyner

**ABSTRACT.** *Mixing models help describe the contribution of liquid, gas, and solid phases to the bulk dielectric permittivity of porous materials. They are particularly useful when studying the electromagnetic properties of the vadose zone using TDR or GPR techniques. The objective of this research was to evaluate the Lichtenecker Mixing Model applied to undisturbed and repacked soil data collected with a 50 MHz impedance sensor. These data along with four different applications of the Lichtenecker Mixing Model were used to predict the  $\alpha$  parameter and/or solid phase permittivity. The four models employed were: (1) the Complex Refractive Index Model,  $\alpha = 0.5$  (CRIM); (2) dual varying of both  $\alpha$  and solid phase permittivity (LI); (3) the direct-weighted average model,  $\alpha = 1$  (DW); and (4) a two-phase simplification of the Lichtenecker model (TM). Overall, the CRIM, LI, and TM models estimated the solid phase permittivity,  $\alpha$ , and soil bulk permittivity within the ranges previously reported in the scientific literature, while the other model proved to be of little practical value. Further validation with glass beads showed that the simple CRIM model was the best predictor for soil bulk permittivity when compared to the two-parameter LI model. A regression model was also developed that accurately predicted the volumetric water content of glass beads from soil bulk permittivity, solid phase permittivity, and porosity.*

**Keywords.** *Complex Refractive Index Model, Lichtenecker, Mixing model.*

**D**ielectric permittivity is an important parameter for indirect determination of water content in partially saturated porous materials using electromagnetic methods (Topp et al., 1980; Campbell, 1990). Among the approaches used for determination of the relationship between the relative permittivity and volumetric water content, the use of purely empirical models (e.g., Topp et al., 1980) and mixing models (Roth et al., 1990) are often found on the literature. Mixing models are a class of models that relate the composite dielectric number of a multiphase mixture to the dielectric numbers and volume fractions of its constituents based on their geometrical arrangement (Roth et al., 1990). Thus, they offer an advantage over purely empirical models in that at least some of the mathematical coefficients involved have a physical meaning.

The dielectric response of partially saturated porous media is known to be frequency dependent (Olhoeft, 1976; Campbell et al., 1990; Roth et al., 1990). There are several designs of sensors on the market with different principles of operations and cost (for example, see Blonquist et al.,

2005, and Vaz et al., 2013, for a comprehensive description and evaluation of sensors). The choice of sensor is often a compromise between cost, frequency of operation, and precision. The Hydra Probe design is based on the work of Campbell (1990). The sensor operates at a fixed frequency of 50 MHz. According to Roth (1990), the most sensitive frequency range for soil water determination lies between 50 MHz and 1 GHz, the lower spectrum showing a stronger dependency on soil type. Besides relatively lower cost when compared to other systems (Blonquist et al., 2005), the Hydra Probe has a smaller probe length, which is more easily implemented in the field and in small laboratory cores, and good accuracy when adequate calibration equations are used (Leão et al., 2010).

## THEORY

The effective or bulk relative permittivity ( $\epsilon_b$ ) of a porous material can be modeled using a class of models known as mixing models, which predict  $\epsilon_b$  based on the individual relative permittivity values for each phase ( $\epsilon_i$ ). One of the simplest forms of mixing models is given by (Zakri et al., 1998):

$$\epsilon_b^\alpha = \sum_{i=1}^n \phi_i \epsilon_i^\alpha \quad (1)$$

where  $\phi_i$  is the volume fraction of each phase ( $\text{cm}^3 \text{cm}^{-3}$ ), and  $\alpha$  is a dimensionless fitting parameter. For partially saturated porous materials with a single liquid phase,  $n = 3$  and equation 1 assumes a form known as the Lichtenecker or Lichtenecker-Rother equation (LI) (Huisman et al.,

---

Submitted for review in April 2014 as manuscript number NRES 10720; approved for publication by the Natural Resources & Environmental Systems Community of ASABE in December 2014.

The authors are **Tairone P. Leão**, Adjunct Professor, Faculdade de Agronomia e Medicina Veterinária, Universidade de Brasília, Brazil; **Edmund Perfect**, Professor, Department of Earth and Planetary Sciences, University of Tennessee, Knoxville, Tennessee; **John S. Tyner** ASABE Member, Associate Professor, Department of Biosystems Engineering and Soil Science, University of Tennessee, Knoxville, Tennessee. **Corresponding author:** Tairone P. Leão, Campus Universitário Darcy Ribeiro, Asa Norte, Brasília, Brazil 70910-970; phone: +55-61-3107-7566; email: tleao@unb.br.

2003; Zakri et al., 1998):

$$\epsilon_b^\alpha = \theta \epsilon_w^\alpha + (1-\phi) \epsilon_s^\alpha + (\phi-\theta) \epsilon_a^\alpha \quad (2)$$

where  $\phi$  is the air-filled porosity of the material ( $\text{cm}^3 \text{cm}^{-3}$ ),  $\theta$  is the volumetric water content ( $\text{cm}^3 \text{cm}^{-3}$ ), and subscripts  $w$ ,  $s$ , and  $a$  represent the water, solid, and air phases, respectively. According to the literature, the  $\alpha$  parameter can vary between -1 and 1, with each end of the range traditionally associated with the equivalent of an electrical circuit wired in parallel ( $\alpha = 1$ ) or in series ( $\alpha = -1$ ).

A special form of equation 2, known as the Complex Refractive Index Model (CRIM), is used to describe isotropic media by setting  $\alpha = 0.5$ :

$$\epsilon_b^{0.5} = \theta \epsilon_w^{0.5} + (1-\phi) \epsilon_s^{0.5} + (\phi-\theta) \epsilon_a^{0.5} \quad (3)$$

This mixing model has been used for estimating the effective permittivity and the individual conductivity of specific phases using time domain reflectometry (TDR) and ground penetrating radar (GPR) techniques (Huisman et al., 2003).

The square root linear calibration equation (SR), which is used as a standard calibration equation for capacitance and TDR sensors, can be viewed as a simplification of equation 3, assuming  $\epsilon_a = 1$  (Huisman et al., 2003):

$$\theta = a\sqrt{\epsilon_b} - b \quad (4)$$

$$\text{where } a = \frac{1}{\sqrt{\epsilon_w} - 1} \text{ and } b = \frac{(1-\phi)\sqrt{\epsilon_s} - \phi}{\sqrt{\epsilon_w} - \phi}$$

However, for practical applications,  $a$  and  $b$  are treated as empirical dimensionless coefficients to be estimated by linear regression. When  $\alpha = 1$ , equation 2 reduces to a direct-weighted (DW) average of the dielectric permittivities of the constituents:

$$\epsilon_b = \theta \epsilon_w + (1-\phi) \epsilon_s + (\phi-\theta) \epsilon_a \quad (5)$$

When  $\alpha = -1$ , equation 3 is analogous to the harmonic weighting of the phases' dielectric permittivities:

$$\frac{1}{\epsilon_b} = \frac{\theta}{\epsilon_w} + \frac{(1-\phi)}{\epsilon_s} + \frac{(\phi-\theta)}{\epsilon_a} \quad (6)$$

Equation 6 is unrealistic, mainly because it implies an inverse relationship between  $\epsilon_b$  and volumetric water content, which is not observed in reality. Experimental research has shown that  $\epsilon_b$  increases with water content, since the permittivity of water is much greater than that of soil or air (Leão, 2009). Therefore, equation 6 was not explored in this research.

Another specific application of equation 2 is for two-phase media (TM), e.g., for a porous medium saturated exclusively with either liquid or gas:

$$\epsilon_b^\alpha = (1-\phi) \epsilon_s^\alpha + \phi \epsilon_f^\alpha \quad (7)$$

where  $\epsilon_f$  is the relative permittivity of the saturating phase, either gas or liquid. Similar theoretical approaches have

been used for calculating effective hydraulic and heat transmission properties in layered media (Pruess, 2004; Zimmerman, 1989).

Criticisms of Lichtenecker-type mixing formulas are available within the scientific literature, one of the most cited being that of Reynolds and Hough (1957) regarding the incorrect assumptions used to derive the theoretical basis of the model. In response, researchers have sought to present corrections to eliminate mathematical inconsistencies (Neelakantaswamy et al., 1985) or theoretical evidence based on the effective medium theory (Zakri et al., 1998), the Maxwell-Garnett equation (Simpkin, 2010), or topology (Goncharenko et al., 2000).

Robinson and Friedman (2003) found the Lichtenecker model to show a poor goodness of fit and a lack of a rigorous theoretical basis. They suggested the Maxwell-Garnett model (MG) for modeling two-phase media. The MG can be written for approximately spherical particles as (Robinson and Friedman, 2003):

$$\epsilon_b = \epsilon_f + 3f \epsilon_f \left( \frac{\epsilon_s - \epsilon_f}{\epsilon_s + 2\epsilon_f - f(\epsilon_s - \epsilon_f)} \right) \quad (8)$$

where  $f = (1 - \phi)$ . Robinson and Friedman (2003) also used the Looyenga model (LO) for comparison purposes (Khan et al., 1986):

$$\epsilon_b^{1/3} = (1-\phi) \epsilon_s^{1/3} + \phi \epsilon_f^{1/3} \quad (9)$$

and a logarithmic linear approximation of the Lichtenecker model (L-LN) with  $\alpha = 0$ , limiting the flexibility of the model for conforming to observational data:

$$\ln \epsilon_b = (1-\phi) \ln \epsilon_s + \ln \phi \epsilon_f \quad (10)$$

In addition to the problem with the flexibility of the L-LN model, Robinson and Friedman (2003) also did not address the physically based evidence for the Lichtenecker model available at the time (Zakri et al., 1998). A topological treatment of the Lichtenecker model can be found in Goncharenko et al. (2000). Furthermore, Simpkin (2010) presented a theoretical derivation of the Lichtenecker model from the Maxwell-Garnett equation.

Overall, the evidence shows that the Lichtenecker model is as effective as, or more effective than, the Maxwell-Garnett equation for predicting the permittivity of multiphase media (Wu et al., 2013; Kiley et al., 2012; Goncharenko et al., 2000). Other models for estimating the complex permittivity of porous materials have been presented by Jones and Friedman (2000) and Kelleners and Verma (2010). However, these models rely on parameters that are difficult to measure or estimate for real soils and therefore are difficult to apply. As pointed out by Neelakantaswamy et al. (1985), the Lichtenecker equation has prevailed because it works well for data from soils across a wide range of materials and applications (Wu et al., 2013; Gnusin et al., 2009; Yang et al., 2009; Batsanov et al., 2008; Chao et al., 2008; Zheng et al., 2005; Roth et al., 1990).

Based on the theoretical premises presented above, our

specific objectives with this research were to: (1) compare the mathematical properties of the Lichtenecker model to those of the Maxwell-Garnett equation, (2) investigate the ranges of estimated solid phase permittivity for three soils with different saturating solutions and disturbance treatments using analytical approaches based on equations 3 to 7, (3) verify the validity of the Complex Refractive Index Model for our data, i.e., the assumption that  $\alpha = 0.5$ , and (4) estimate  $\alpha$  with the Lichtenecker model (eq. 2) and assess its ability to differentiate between different soils, saturating solutions, and disturbance treatments.

## MATERIALS AND METHODS

Thirty minimally disturbed soil cores (hereafter referred to as “undisturbed”) and three bulk soil samples were collected on 10 June 2005 at the Plant Sciences experimental farm at the University of Tennessee, Knoxville. The sampling was performed in areas with different soil series, covering three contrasting soil textural classes, according to the USDA system: clay (fine-loamy, siliceous, semiactive, thermic Typic Paleudult), sandy loam (fine-loamy, siliceous, semiactive, thermic Humic Hapludult), and silty clay loam (fine-silty, mixed, active, mesic Fluvaquentic Eutrudept) (table 1).

The undisturbed cores (5.37 cm inner diameter  $\times$  6 cm long) were collected using a Uhland core sampler. The bulk disturbed samples were collected with a shovel; approximately 5 kg of soil was obtained for each soil type. All samples were collected at a depth of 20 to 25 cm. The bulk soil samples were air dried, broken apart by hand, sieved with a 2 mm mesh sieve, and packed to give ten “disturbed” cores for each soil texture. The disturbed cores were the same size as the undisturbed cores. The average bulk densities of the disturbed and undisturbed soil samples are presented in table 1.

Duplicate samples of the disturbed and undisturbed cores were slowly saturated for three days, from the bottom up, with saline solutions at five concentrations: distilled-deionized water ( $\sim 0$  or control), KCl at 0.01 and 0.02 mol L<sup>-1</sup>, and CaCl<sub>2</sub> at 0.01 and 0.02 mol L<sup>-1</sup>. A Hydra Probe sensor (Stevens, 2007) was inserted into the top end of each sample. The samples were then placed horizontally on load cells (model LSP-1, Transducer Techniques, Temecula, Cal.), and the Hydra Probes and load cells were connected to dataloggers (Vitel VX1100, Stevens Water Monitoring Systems, Portland, Ore., and 21X Micrologger, Campbell Scientific, Logan Utah, respectively). The real component

of bulk soil relative permittivity ( $\epsilon_b$ ) was measured with the Hydra Probe, while the load cells measured loss in water mass due to air drying. All measurements were recorded in 5 min intervals. After approximately five days of air drying (21.5°C, CV = 5.24%), when there was minimal change in mass with time, the probes were removed from the soil samples. The remaining gravimetric water content of the soils was then measured by oven drying at 105°C for 24 h (Klute, 1986). The  $\epsilon_b$  measurements were temperature corrected (Stevens, 2007).

Evaluation of models was also performed using an independent dataset collected in the same manner as described previously, but with glass beads instead of soil. The glass beads had average diameters of 2.0, 1.0, 0.5, 0.25, 0.125, and 0.0625 mm and a particle density of 2.5 g cm<sup>-3</sup> (Mo-Sci Corp., Rolla, Mo.). Disturbed samples were made up by mixing the glass beads fractions in different proportions: 44%, 25%, 15%, 8%, 5%, and 3% (one sample); 30%, 23%, 17%, 13%, 10%, and 7% (two samples); 23%, 20%, 17%, 15%, 13%, and 12% (one sample), and 20%, 18%, 17%, 16%, 15%, and 14% (one sample), respectively. The bulk densities for these disturbed glass beads cores were: 1.78, 1.85, 1.80, 1.81, and 1.82 g cm<sup>-3</sup>, respectively. The glass beads samples were saturated with distilled-deionized water only.

The relative permittivity of the air ( $\epsilon_a$ ) was assumed to be unity (Kraus, 1992), while that of the solution ( $\epsilon_s$ ) was approximated by immersing the Hydra Probes in each solution, resulting in values of: 84 for distilled-deionized water, 77.9 and 82.4 for KCl at 0.01 and 0.02 mol L<sup>-1</sup>, and 77.9 and 82.2 for CaCl<sub>2</sub> at 0.01 and 0.02 mol L<sup>-1</sup>, respectively. Equations 2 through 7 were fitted to the data by nonlinear regression to estimate the  $\alpha$  and  $\epsilon_s$  coefficients, and by linear regression to estimate coefficients  $a$  and  $b$  (Bates and Watts, 1988). The fitted coefficients were then used as independent variables in analysis of variance (ANOVA) models to check if they differed among the soil, solution, and disturbance treatments (Doncaster and Davey, 2007). All statistical analyses were performed using SAS statistical analysis software (SAS, 2004).

## RESULTS AND DISCUSSION

### MATHEMATICAL PROPERTIES OF LICHTENECKER AND MAXWELL-GARNETT MODELS

Following the approach suggested by Robinson and Friedman (2003) and using ( $\epsilon_b$ ,  $\epsilon_f$ ) data pairs found in their research, i.e., (3.7, 1), (5, 2.7), (6.5, 6), (8, 10), (14, 27.9),

Table 1. Soil physicochemical properties.<sup>[a]</sup>

Soil	Sand (%)	Silt (%)	Clay (%)	Total C (%)	pH (H <sub>2</sub> O)	Bulk Density		Particle Density (g cm <sup>-3</sup> )	Hydraulic Conductivity		SSA <sup>[b]</sup> (m <sup>2</sup> g <sup>-1</sup> )
						Undist. (g cm <sup>-3</sup> )	Dist. (g cm <sup>-3</sup> )		Undist. (cm s <sup>-1</sup> )	Dist. (cm s <sup>-1</sup> )	
Clay	20.35	34.06	45.59	0.135 (0.010)	5.1	1.45 (0.04)	1.30 (0.02)	2.731 (0.008)	3.00×10 <sup>-5</sup> (4.27×10 <sup>-5</sup> )	3.24×10 <sup>-3</sup> (1.31×10 <sup>-3</sup> )	34.678 (0.007)
Silty clay loam	13.03	52.59	34.38	0.866 (0.019)	6.2	1.46 (0.02)	1.31 (0.01)	2.669 (0.004)	3.62×10 <sup>-3</sup> (5.85×10 <sup>-3</sup> )	1.85×10 <sup>-3</sup> (4.76×10 <sup>-4</sup> )	16.389 (0.337)
Sandy loam	74.41	19.32	6.27	0.233 (0.007)	6.0	1.65 (0.02)	1.55 (0.02)	2.685 (0.005)	5.79×10 <sup>-4</sup> (7.00×10 <sup>-4</sup> )	4.71×10 <sup>-3</sup> (4.40×10 <sup>-3</sup> )	2.176 (0.056)

<sup>[a]</sup> Standard deviations of mean estimates are shown in parentheses.

<sup>[b]</sup> SSA = specific surface area.

(20, 49), (22.8, 58.3), and (28.5, 79), the suitabilities of the TM, MG, LO, and L-LN models (eqs. 7 through 10) were preliminarily assessed assuming a solid phase permittivity of 7.6 and porosity of 0.395 (fig. 1). The 1:1 line of  $\epsilon_b$  versus  $\epsilon_f$  is also presented. The interception point of a best fit of the observed data with this line corresponds to the value of the solid phase permittivity (Robinson and Friedman, 2003). Figure 1 shows that the TM and MG equations fit the data the best. The Lichtenecker model evaluated by Robinson and Friedman (2003) was a logarithmic linear approximation without taking into account the  $\alpha$  parameter (L-LN). When  $\alpha$  is allowed to vary, the fitting properties of the model are significantly improved. The better accuracy of the TM model can be confirmed by using the root mean square error (RMSE) as a goodness of fit indicator (fig. 1). If  $\alpha$  is left to vary in the Lichtenecker equation, the RMSE drops to 0.42 and the optimized  $\alpha$  value is 0.5785.

The independence of the solid phase permittivity from the porosity when the effective permittivity is equal to the background permittivity described for the MG model by Robinson and Friedman (2003) is also valid for the TM model regardless of the  $\alpha$  value chosen. This is demonstrated in figure 2, where equation 7 was used to predict  $\epsilon_b$  for a range of  $\epsilon_f$  values by setting  $\alpha = 5$  and using three values of  $f = (1 - \phi)$ : 0.2, 0.4, and 0.6. These results show that the Lichtenecker model can also be used to estimate the solid phase permittivity using the immersion method.

The major advantage of the Lichtenecker model over the Maxwell-Garnett and other models is that it is a three-phase model and thus can be used to estimate the effective permittivity of unsaturated media, including gas and liquid phases. Data analysis using the three-phase Lichtenecker and CRIM models is presented in the following sections.

#### LICHTENECKER MODEL WITH FITTED $\alpha$ AND $\epsilon_s$ VALUES

When both coefficients from equation 2 ( $\epsilon_s$  and  $\alpha$ ) were estimated by nonlinear regression, convergence was not achieved for all of the soil samples. The nonlinear estimation procedure failed to converge in 20% of the clay soil

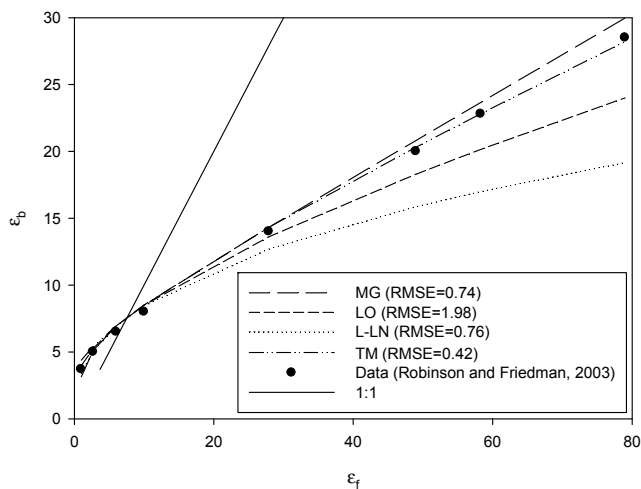


Figure 1. Effective permittivity as a function of fluid permittivity predicted by the Maxwell-Garnett (MG), Looyenga (LO), Lichtenecker-ln (L-LN), and Lichtenecker- $\alpha$  (TM) models.

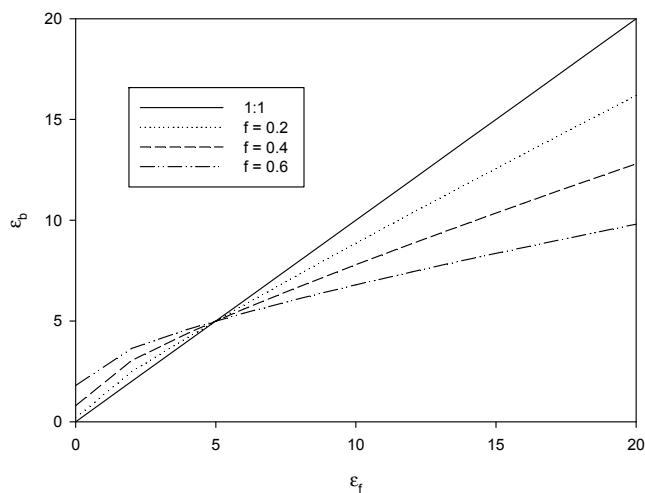
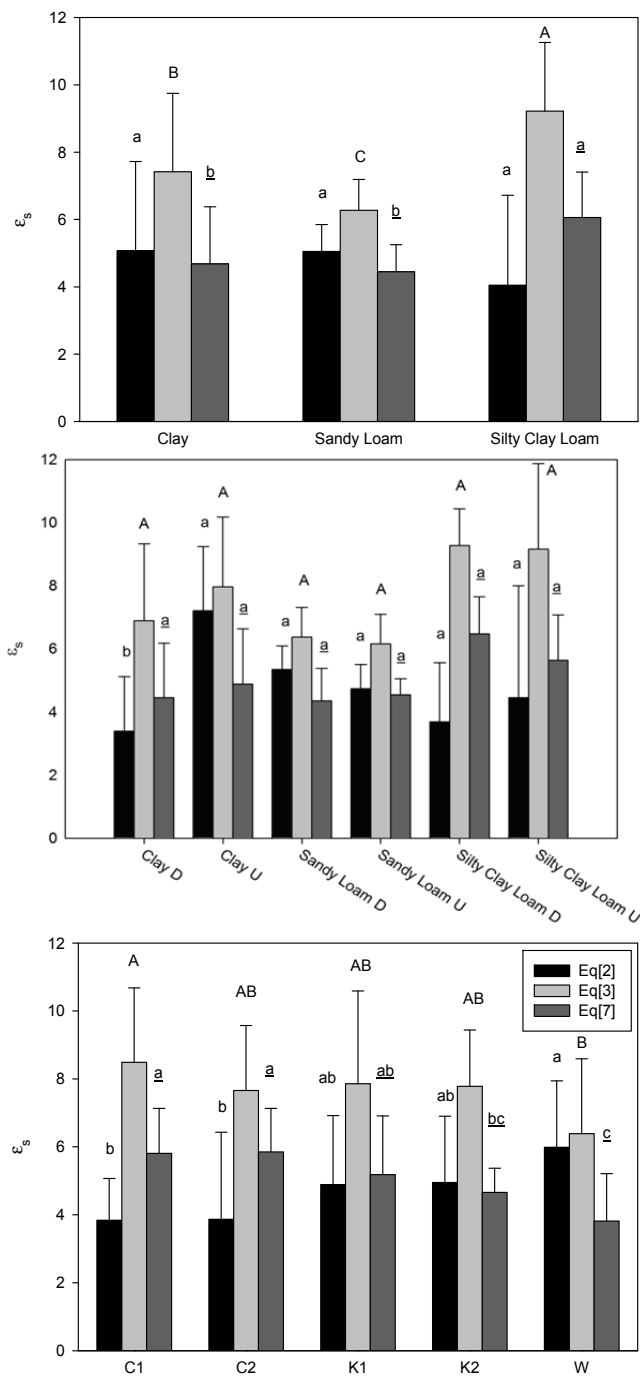


Figure 2. Effective permittivity as a function of fluid permittivity predicted by the Lichtenecker- $\alpha$  (TM) model for three  $f = (1 - \phi)$  values with  $\epsilon_s = 5$ .

samples and in 40% of the silty clay loam soil samples, even though a robust fitting algorithm and a larger number of iterations were used. Convergence problems are exacerbated by adding parameters to a nonlinear model, resulting in the model having more parameters than necessary to fit the data, or when the model does not match the shape of the data. For the remaining samples, all of the fits were statistically significant ( $\text{Pr} > F < 0.0001$ ), with average, minimum, and maximum  $R^2$  values of 0.99, 0.96, and 0.99, respectively. The average (and standard deviation) values for the estimated  $\epsilon_s$  for each soil are presented in figure 3. The average values discussed above were initially presented by soil type because it was expected that both  $\epsilon_s$  and  $\alpha$  would primarily be a function of soil type, being directly influenced by clay content and mineralogy. To assess if the estimated coefficients were influenced by other variables, an ANOVA was performed with the coefficients estimated from equation 2 as independent variables and soil, disturbance, and saturating solution treatment and their interactions as class variables. The resulting ANOVAs were significant for both  $\epsilon_s$  ( $\text{Pr} > F = 0.0031$ ) and  $\alpha$  ( $\text{Pr} > F = 0.0034$ ). For  $\epsilon_s$  estimated from equation 2, the only significant factors were disturbance and the soil versus disturbance interaction. This indicates the need for comparing disturbance treatments within a soil (fig. 3).

Comparison of means was performed using the least significant difference (LSD) test (Webster, 2007). For textural classes analyzed individually, only samples of the clay soil were statistically different between the disturbance treatments (fig. 3). The  $\epsilon_s$  values for the disturbed and undisturbed samples were not statistically different for the silty clay loam and sandy loam soils. Overall, the average  $\epsilon_s$  was slightly higher for undisturbed conditions than for disturbed conditions (fig. 3). The difference between disturbance treatments for the clay samples is probably related to a mixed soil effect, since it is expected that within the same soil the effect of packing should not significantly affect the  $\epsilon_s$  estimates, as was observed for the other two soils.



**Figure 3.** Average solid phase permittivity for each soil fitted using equations 2, 3, and 7 for soils (top), soil and disturbance (middle), and salt solutions (bottom). Error bars represent standard deviations of estimates. Means followed by the same letter are not significantly different (LSD,  $p = 0.05$ ). Lowercase letters compare estimates from equation 2, uppercase letters compare estimates from equation 3, and underlined letters compare estimates from equation 7. C1 =  $\text{CaCl}_2$   $0.01 \text{ mol L}^{-1}$ , C2 =  $\text{CaCl}_2$   $0.02 \text{ mol L}^{-1}$ , K1 =  $\text{KCl}$   $0.01 \text{ mol L}^{-1}$ , K2 =  $\text{KCl}$   $0.02 \text{ mol L}^{-1}$ , and W = distilled-deionized water.

The  $\alpha$  parameter estimated by the nonlinear regression procedure varied from 0.33 to 0.90, with average and standard deviation values of 0.60 and 0.13, respectively. The estimated values were within the ranges of +1 and -1 reported for this parameter, and the average was close to the value of 0.5 used in the CRIM equation, indicating that

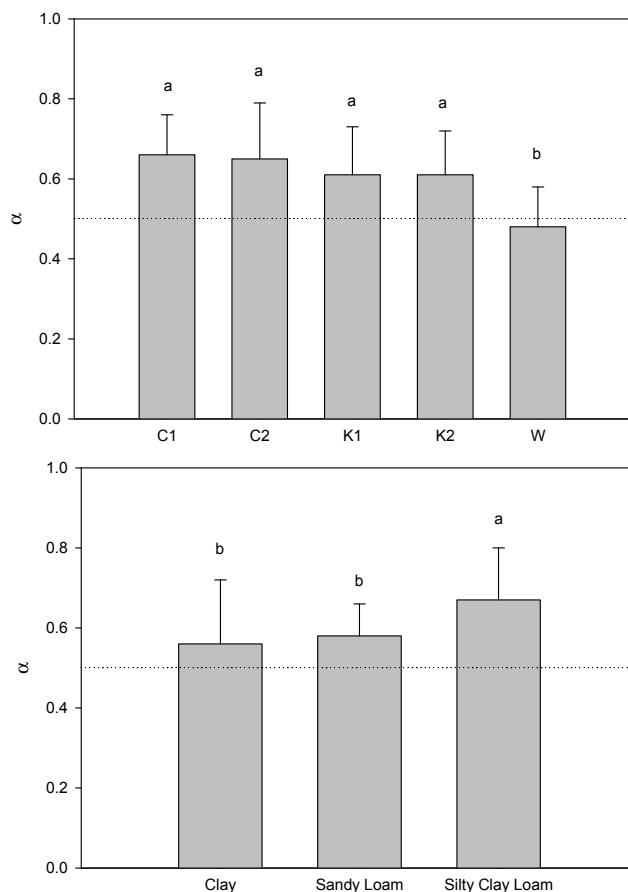


**Figure 4.** Average  $\alpha$  values for each salt solution (top) and soil (bottom) fitted using equation 2. Error bars represent standard deviations of estimates. Means followed by the same letter are not significantly different (LSD,  $p = 0.05$ ). C1 =  $\text{CaCl}_2$   $0.01 \text{ mol L}^{-1}$ , C2 =  $\text{CaCl}_2$   $0.02 \text{ mol L}^{-1}$ , K1 =  $\text{KCl}$   $0.01 \text{ mol L}^{-1}$ , K2 =  $\text{KCl}$   $0.02 \text{ mol L}^{-1}$ , and W = distilled-deionized water. Dotted line indicates  $\alpha = 0.5$ .

the soils under evaluation were close to isotropic. The  $\alpha$  and  $\epsilon_s$  parameters from equation 2 were highly correlated ( $r = -0.89$ ,  $\text{Pr} > |r| < 0.0001$ ), indicating a potential over-parameterization in this model.

ANOVA performed on the  $\alpha$  parameter estimates indicated significant effects due to soil and saturating solution. Averages for the silty clay loam were higher and statistically different from the averages for the sandy loam and clay soils, which were not statistically different following the LSD test (fig. 4). Regarding the saturating solutions, only the distilled-deionized water average was statistically different from the salt solutions (fig. 4). Although not significant, the average  $\alpha$  value for undisturbed conditions was closer to 0.5 than that for the disturbed samples, indicating that the undisturbed media had a higher degree of isotropy. It is possible that the packing process introduced a degree of anisotropy into the disturbed samples. Roth et al. (1990) also found  $\alpha$  values close to 0.5, indicating that the Lichtenecker model when applied to real soil data tends to be close to the CRIM model.

#### COMPLEX REFRACTIVE INDEX MODEL (CRIM)

Data from the drying experiments for each soil core were also fitted to equation 3 using nonlinear regression.

The ANOVA from the nonlinear regression procedures showed that all of the fittings were statistically significant ( $\text{Pr} > F < 0.0001$ ). The default nonlinear regression convergence criterion was also met in all cases. The average coefficient of determination ( $R^2$ ) was 0.98, with a minimum of 0.96 and a maximum of 0.99. The average (with standard deviation in parentheses) predicted solid phase permittivity ( $\epsilon_s$ ) is presented in figure 3. The  $\epsilon_s$  values estimated using equation 2 were significantly different from those estimated using equation 3 ( $\text{Pr} > |t| < 0.0001$ ).

ANOVA for the  $\epsilon_s$  values estimated using the CRIM model (eq. 3) was also performed using soil, disturbance, salt solution, and their interactions as independent factors. The resulting model was statistically significant ( $\text{Pr} > F < 0.0001$ ). However, of the three class factors included, only soil texture was significant. An evaluation of the  $\epsilon_s$  values using the LSD test showed that the all soil averages were statistically different, decreasing in the order silty clay loam > clay > sandy loam (fig. 3).

The solid phase permittivity of common soil minerals was evaluated by Robinson (2004). The  $\epsilon_s$  of quartz was estimated to be 4.4 ( $\pm 0.3$ ), while that of phyllosilicate minerals was slightly higher. Kaolinite had an average  $\epsilon_s$  of 5.1 ( $\pm 0.7$ ), and biotite mica had an average  $\epsilon_s$  of 6.0 ( $\pm 0.5$ ), while the 2:1 grade minerals illite and montmorillonite had  $\epsilon_s$  values of 5.8 ( $\pm 0.2$ ) and 5.5 (standard deviation not presented), respectively (Robinson, 2004). For equation 3, the sandy loam soil had an estimated  $\epsilon_s$  value that was higher than the value measured for quartz by Robinson (2004). It was expected that the average values for the silty clay loam and clay soils would be higher than the value for the sandy loam soil due to the presence of 2:1 soil minerals (vermiculite, illite, and mica) and kaolinite, which should increase the permittivity of the soil. The mineralogy of the clay soil is composed of 8% kaolinite and 9.2% of combined vermiculite, illite, and mica; the silty clay loam soil has 3.7% kaolinite and 9.7% of combined vermiculite, illite, and mica, while the sandy loam soil has 1.2% kaolinite and 5.1% of combined vermiculite, illite, and mica, all on a mass basis (Leão, 2009). The proportions of the 2:1 soil minerals in the three soils investigated agree with the ranking of the estimates of  $\epsilon_s$  from equation 3 for the silty clay loam and clay soils.

The  $\epsilon_s$  values estimated using equation 2 were lower than those from equation 3 and closer to the values measured by Robinson (2004). For equation 2, the clay soil had the highest average values for  $\epsilon_s$ , and the silty clay loam had the lowest (fig. 3). It is possible that this was caused by compensation between  $\alpha$  and  $\epsilon_s$  in the fitting procedure, as both parameters were estimated using nonlinear regression, and thus the flexibility of  $\alpha$  might have caused  $\epsilon_s$  to assume values not representative of the mineralogical composition of the samples. For equations 2 and 3, the  $\epsilon_s$  values were also close to the ranges reported for soils and minerals by Cassidy (2009), Zheng et al. (2005), and Kraus (1992), indicating that inverse modeling of mixing models is an effective tool for estimating solid phase permittivity.

## SQUARE ROOT LINEAR MODEL

The theoretical approach of Huisman et al. (2003) states that the fitting coefficients  $a$  and  $b$  in equation 4 can be correlated to  $\epsilon_s$ ,  $\epsilon_w$ , and  $\phi$ . This assumption was tested by fitting equation 4 to the data from this study using linear regression and estimating  $a$  and  $b$  for each soil sample. The estimated coefficients were then tested as (Huisman et al., 2003):

$$a = \frac{1}{\sqrt{\epsilon_w} - 1} \text{ and } b = \frac{(1-\phi)\sqrt{\epsilon_s} - \phi}{\sqrt{\epsilon_w} - \phi}$$

and the suitability of these relationships was evaluated statistically. The  $\epsilon_s$  values estimated with equation 3 were used in the calculations for simplicity. The  $a$  parameter

estimated from regression was not correlated with  $\frac{1}{\sqrt{\epsilon_w} - 1}$

( $r = -0.09$ ,  $\text{Pr} > |r| = 0.51$ ), while  $b$  was significantly corre-

lated with  $\frac{(1-\phi)\sqrt{\epsilon_s} - \phi}{\sqrt{\epsilon_w} - \phi}$  ( $r = 0.54$ ,  $\text{Pr} > |r| < 0.0001$ ), indi-

cating that there is a relationship between  $b$  and  $\epsilon_s$ ,  $\epsilon_w$  and  $\phi$  as proposed by Huisman et al. (2003). To test these relationships further,  $a$  and  $b$  were regressed against  $\epsilon_s$ ,  $\epsilon_w$ , and  $\phi$  using multiple linear regression. The resulting models were:

$$a = 0.0904 + 0.1411\phi - 0.0046\epsilon_s \quad (11)$$

$$b = -0.1281 - 0.3424\phi + 0.0081\epsilon_s \quad (12)$$

The ANOVA from the regression indicates that both regression models were significant ( $\text{Pr} > F < 0.0001$ ). Equation 11 had a coefficient of determination ( $R^2$ ) of 0.70, and equation 12 had an  $R^2$  value of 0.32. Neither  $a$  nor  $b$  were significantly related to  $\epsilon_w$  following regression analysis.

By substituting equations 11 and 12 into equation 4, it is possible to generate a semi-empirical model for predicting  $\theta$  from  $\epsilon_b$  that incorporates the effects of porosity (and conversely bulk density) and the solid phase permittivity:

$$\theta = \sqrt{\epsilon_b} (0.0904 + 0.1411\phi - 0.0046\epsilon_s) + (-0.1281 - 0.3424\phi + 0.0081\epsilon_s) \quad (13)$$

Initially, the overall precision of equation 13 was assessed for the disturbed and undisturbed soil samples by evaluating the relationship between predicted and observed values of  $\theta$ . The  $R^2$  value for the scatterplot of known versus predicted  $\theta$  values (eq. 13) was 0.98, with an RMSE of  $0.0289 \text{ cm}^3 \text{ cm}^{-3}$  (fig. 5). This indicates that there is a very good agreement between the observed and estimated water content values using equation 13. Since the model was not tested using an independent soil dataset, its validity cannot be extrapolated for other soils and conditions. However, it is likely that the validity of the influence of  $\epsilon_s$  and  $\phi$  in the estimated  $\theta$  values will still hold in other soils and conditions, and thus the necessity of finding accurate and simple methods of estimating  $\epsilon_s$ .

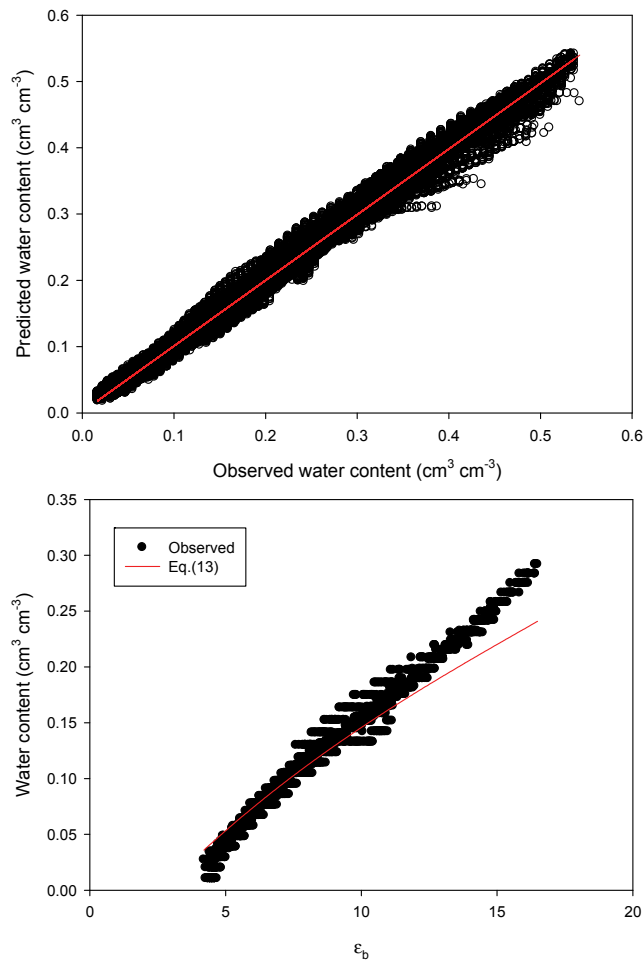


Figure 5. Predicted vs. observed volumetric water contents for the whole soils dataset (top) and predicted and observed volumetric water contents vs.  $\epsilon_b$  for glass beads data (bottom). Predicted values were estimated using equation 13.

#### DIRECT WEIGHTED AVERAGE MODEL

The direct-weighted average model (eq. 5) was fitted to the soil data with a single adjusting coefficient, the solid phase permittivity ( $\epsilon_s$ ). As a result, the nonlinear fitting was straightforward, and convergence was achieved for all 60 soil samples. All of the fits were significant ( $\text{Pr} > F < 0.0001$ ), with average, minimum, and maximum  $R^2$  values of 0.99, 0.98, and 0.99, respectively. The main issue with the DW model is that it yielded negative values for  $\epsilon_s$  for all but two of the samples. Negative values have no physical meaning for  $\epsilon_s$  and are a mathematical artifact. Applying measured  $\epsilon_w$  values, the slope of equation 5 becomes equal to  $(\epsilon_w - 1)$ , and thus it is constant for each salt treatment. The only fitting parameter ( $\epsilon_s$ ) is incorporated in the intercept as  $\epsilon_s(1 - \phi) + \phi$ . Despite their negative signs, the estimated  $\epsilon_s$  values were used for further analysis in order to assess the suitability of this parameter for differentiating among soils, disturbance, and salt solutions. The ANOVA results showed that only soil and disturbance were significant factors ( $\text{Pr} > F < 0.0001$ ), with average estimated  $\epsilon_s$  values (with standard deviations in parentheses) of -10.96 ( $\pm 4.54$ ), -7.25 ( $\pm 3.79$ ), and -4.28 ( $\pm 2.47$ ) for the clay, silty clay loam, and sandy loam soils, respectively. Since the

values have a negative sign, they are not shown alongside the results from the other models in the graphs. The average  $\epsilon_s$  values were -8.94 ( $\pm 2.47$ ) for disturbed and -6.04 ( $\pm 2.47$ ) for undisturbed samples. Regarding grain size distribution,  $\epsilon_s$  decreased with increasing clay content, following a different trend from that observed with equations 2 and 3.

#### TWO-PHASE MEDIA MODEL

The TM model presented in equation 7 is a simplification of the Lichtenecker model (eq. 2) for when the soil is completely saturated with solution (i.e.,  $\theta = \phi$ ) or completely dry. As neither of these scenarios can be adequately achieved for real soils, the theory behind the model is an approximation to real conditions.

To estimate  $\epsilon_s$  with equation 7, the measured  $\epsilon_w$ ,  $\theta_s$ , and  $\epsilon_b$  were inputted in the equation with the assumptions that  $\alpha = 0.5$  and  $\theta_s = \phi$ . The  $\epsilon_s$  was then calculated numerically using a spreadsheet goal-seeking algorithm. Results for equation 7 with  $\alpha$  set to 1 or -1 are not presented, since they yielded negative or unreasonably high values for  $\epsilon_s$ . The average estimated  $\epsilon_s$  values were statistically different for soils and saturating solutions according to ANOVA ( $\text{Pr} > F < 0.0001$ ). Regarding soils,  $\epsilon_s$  was expected to be different, as the samples differed in their mineralogy. Averages for clay and sandy loam samples did not differ statistically following the LSD test at 5% probability level (fig. 3). The estimates of  $\epsilon_s$  from equation 7 were closer to those from equation 2 than those from equation 3 (fig. 3). The values were also close to measured values of solid phase permittivity of real soil constituents (Robinson, 2004).

Regarding the different salt solutions, average values of  $\epsilon_s$  decreased from samples saturated with  $\text{CaCl}_2$  at higher concentration to samples saturated with distilled-deionized water (fig. 3). The statistical comparison between averages from LSD testing is presented in figure 3. Averages were higher for samples saturated with  $\text{CaCl}_2$  and lower for samples saturated with distilled-deionized water, while samples saturated with KCl were intermediate. There was no statistical difference between disturbed and undisturbed samples. The ionic strength of the saturating solution influenced the estimated values of  $\epsilon_s$  using equation 7 with  $\alpha$  fixed to 0.5. Although the solid phase permittivity should be constant and independent of the saturating solution, it appears that the presence of the salt solutions changed the interaction between the solid phase and the saturating solution, altering the estimated  $\epsilon_s$  values. This effect could be related to changes in surface electrical properties associated with changes in the diffuse electrical double layer when different salts are present in the bulk solution.

#### MODEL VALIDATION WITH GLASS BEADS

Equations with adequate estimates of  $\alpha$  and  $\epsilon_s$  and with better fitting properties, namely equations 2, 3, and 13 (based on eq. 4) were selected for validation with the glass beads drying data. The  $\epsilon_s$  and  $\alpha$  parameters for the sandy loam soil were used in the models for estimating  $\epsilon_b$  and  $\theta$  since the glass beads used in the experiment were coarse grained, i.e., particle diameters greater than 0.0625 mm,

and had a similar mineralogy. Equation 13 was used to estimate water content with  $\epsilon_s$  estimated for sandy loam soil using equation 3, while total porosity was calculated from the sample bulk densities and the particle density given by the manufacturer. Since the glass beads samples were coarse grained, the range of water content and the  $\epsilon_b$  values were relatively low (fig. 5). The model was most accurate for low values of  $\theta$  and  $\epsilon_b$  and underestimated the values of  $\theta$  at high values of  $\epsilon_b$ . Despite this deviation, the coefficient of determination ( $R^2$ ) for predicted versus estimated  $\theta$  values using equation 13 for the glass beads data was 0.98, and the RMSE was  $0.0155 \text{ cm}^3 \text{ cm}^{-3}$ . The RMSE was close to that of soil-specific models developed in previous research (Leão et al., 2010).

Equations 2 and 3 were used to predict  $\epsilon_b$  using the coefficients estimated for the sandy loam soil,  $\epsilon_s = 5.01$  and  $\alpha = 0.59$  for equation 2 and  $\epsilon_s = 6.30$  for equation 3. The resulting predicted versus observed relationships are shown in figure 6. It can be seen that equation 2 tended to overestimate the higher values of  $\epsilon_b$ , while results for equation 3 (CRIM) were very close to a 1:1 relationship. The lower RMSE value

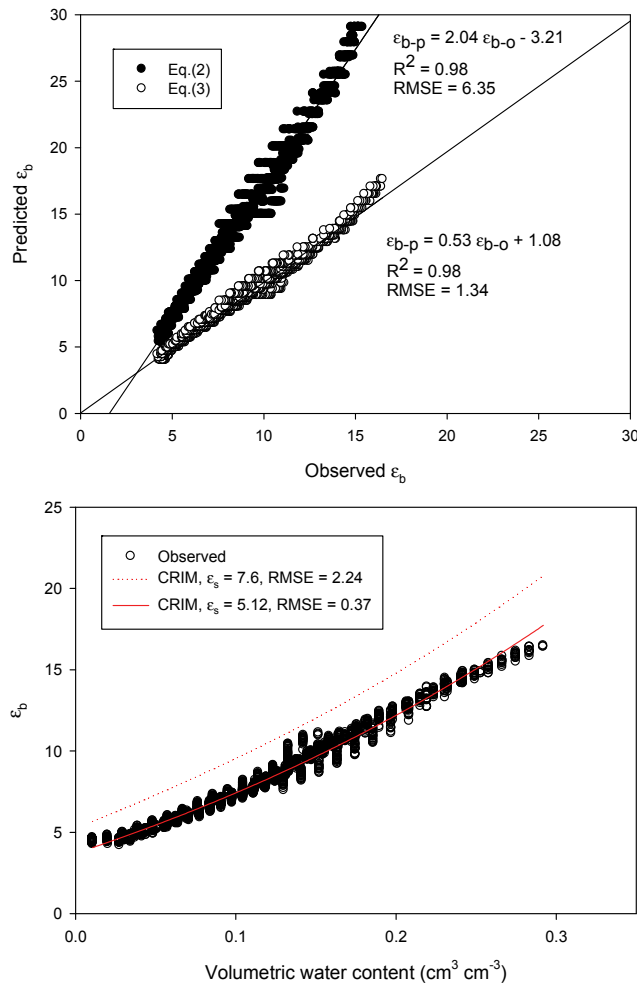


Figure 6. Predicted vs. observed  $\epsilon_b$  values estimated using equations 2 and 3 for glass beads samples (top) and effective permittivity as a function of volumetric water content (bottom). Predictions using the CRIM model with  $\epsilon_s = 5$  and  $\epsilon_s = 7.6$  are shown for comparison. Subscripts  $o$  and  $p$  are for observed and predicted values, respectively.

for equation 3 is presented in figure 6, validating the better performance of the CRIM model in terms of accuracy over the general Lichtenecker two-parameter model. These results show that the CRIM model has a better predictive performance than models where  $\alpha$  is allowed to vary.

The glass beads data were also used to evaluate effective permittivity predictions using the CRIM model with solid phase permittivity values found in this research and from the literature and  $\alpha = 0.5$  (fig. 6). Predictions of effective permittivity for glass beads using the value of solid phase permittivity reported by Robinson and Friedman (2003),  $\epsilon_s = 7.6$ , resulted in an RMSE value of 2.24 when the CRIM was used and 1.13 when the value found by nonlinear fitting for the sandy loam data was used,  $\epsilon_s = 6.30$ . Using a fitted value of  $\epsilon_s = 5.12$  resulted in the lowest RMSE value (0.37), indicating that the permittivity of these glass beads was likely lower than the value of 7.6 reported by Robinson and Friedman (2003) (fig. 6).

## CONCLUSIONS

The Lichtenecker model performed better than the Maxwell-Garnett model to predict effective permittivity of two-phase media. The main advantages of the Lichtenecker model are that it is mathematically simple and can be expanded to unsaturated soils or other three-phase media. The use of mixing models and inverse modeling via nonlinear regression can be a useful approach for estimating soil electromagnetic properties. Of the equations evaluated in this research, the Complex Refractive Index Model ( $\alpha = 0.5$ ) and the Lichtenecker equation with  $\alpha$  and  $\epsilon_s$  as fitting parameters had a better predictive performance and produced estimates of  $\alpha$  and  $\epsilon_s$  closer to values reported for soil materials than other models, namely the Lichtenecker model with  $\alpha = 1$  or  $\alpha = -1$ . Negative values of  $\alpha$  might not be realistic for real soil conditions. The two-phase simplification of the Lichtenecker model also predicted  $\epsilon_s$  values close to the ranges expected for soil materials. A new semi-empirical model (based on mixing model theory) was developed using multiple regression analysis and evaluated for predicting volumetric water content from bulk permittivity,  $\epsilon_s$ , and porosity. This model showed accurate results when validated using glass beads data and when compared to data from previous research. Overall, our results show that the simpler CRIM equation with a single fitting parameter ( $\epsilon_s$ ) and  $\alpha = 0.5$  had a better and more realistic capability for predicting  $\epsilon_b$  than the other models evaluated.

## ACKNOWLEDGEMENTS

This research was funded in part by the U.S. Army Corps of Engineering, Engineering Research and Development Center (Contract No. BR05-0001C, UT-USACE/ERDC).

## REFERENCES

Bates, D. M., & Watts, D. G. (1988). *Nonlinear Regression Analysis and its Application*. Hoboken, N.J.: John Wiley and Sons.



- Batsanov, S. S., Poyarkov, K. B., & Gavrilkin, S. M. (2008). Oriental polarization of molecular liquids in contact with diamond crystals. *ETP Letters*, 88(9), 595-596. <http://dx.doi.org/10.1134/S0021364008210108>.
- Blonquist, J. M., Jones, S. B., & Robinson, D. A. (2005). Standardizing characterization of electromagnetic water content sensors: Part 2. Evaluation of seven sensing systems. *Vadose Zone J.*, 4(4), 1059-1069.
- Campbell, J. E. (1990). Dielectric properties and influence of conductivity in soils at one to fifty megahertz. *SSSA J.*, 54(2), 332-341. <http://dx.doi.org/10.2136/sssaj1990.03615995005400020006x>.
- Cassidy, N. (2009). Ground penetrating radar: Theory and applications. In *Ground Penetrating Radar: Data Processing, Modeling, and Analysis* (pp. 141-249. Amsterdam, The Netherlands: Elsevier.
- Chao, F., Liang, G., Kong, W., Zhang, Z., & Wang, J. (2008). Dielectric properties of polymer/ceramic composites based on thermosetting polymers. *Polymer Bulletin*, 60(1), 129-136. <http://dx.doi.org/10.1007/s00289-007-0840-3>.
- Doncaster, C. P., & Davey, J. H. (2007). *Analysis of Variance and Covariance: How to Choose and Construct Models for the Life Sciences*. Cambridge, U.K.: Cambridge University Press.
- Gnusin, N. P., Demina, O. A., & Annikova, L. A. (2009). Method of parameter calculation of ion-exchange resins. *Russian J. Electrochem.*, 45(4), 490-495. <http://dx.doi.org/10.1134/S1023193509040211>.
- Goncharenko, A. V., Lozovski, V. Z., & Venger, E. F. (2000). Lichtenecker's equation: Applicability and limitations. *Optics Comm.*, 174(1-4), 19-32. [http://dx.doi.org/10.1016/S0030-4018\(99\)00695-1](http://dx.doi.org/10.1016/S0030-4018(99)00695-1).
- Huisman, J. A., Hubbard, S. S., Redman, J. D., & Annan, A. P. (2003). Measuring soil water content with ground penetrating radar: A review. *Vadose Zone J.*, 2(4), 476-491. <http://dx.doi.org/10.2136/vzj2003.4760>.
- Jones, S. B., & Friedman, S. P. (2000). Particle shape effects on the effective permittivity of anisotropic or isotropic media consisting of aligned or randomly oriented ellipsoidal particles. *Water Resource Res.*, 36(10), 2821-2833. <http://dx.doi.org/10.1029/2000WR900198>.
- Kelleners, T. J., & Verma, A. K. (2010). Measured and modeled dielectric properties of soils at 50 megahertz. *SSSA J.*, 74(3), 744-752. <http://dx.doi.org/10.2136/sssaj2009.0359>.
- Khan, K. M., Shamin, A., & Shah, M. A. (1986). Application of Looyenga's equation at low frequencies. *Materials Sci. Letters*, 5(9), 845-846. <http://dx.doi.org/10.1007/BF01729246>.
- Kiley, E. M., Yakovlev, V. V., Ishizaki, K., & Vaucher, S. (2012). Applicability study of classical and contemporary models for effective complex permittivity of metal powders. *J. Microwave Power Electromag. Energy*, 46(1), 26-38.
- Klute, A. (1986). Water retention: Laboratory methods. In A. Klute (Ed.), *Methods of Soil Analysis: Part 1* (2nd ed., pp. 635-660). Madison, Wis.: ASA and SSSA.
- Kraus, J. D. (1992). *Electromagnetics*. New York, N.Y.: McGraw-Hill.
- Leão, T. P. (2009). Effects of water content and salinity on soil electrical properties at 50 MHz: Structural and textural interactions. PhD diss. Knoxville, Tenn.: University of Tennessee.
- Leão, T. P., Perfect, E., & Tyner, J. S. (2010). Estimation of soil water content using a 50 MHz impedance sensor: Soil texture, structure, and salinity interactions. *Trans. ASABE*, 53(1), 163-170. <http://dx.doi.org/10.13031/2013.29510>.
- Neelakantaswamy, P. S. (1985). Complex permittivity of a dielectric mixture: Corrected version of Lichtenecker's logarithmic law of mixing. *Electronics Letters*, 21(7), 270-271. <http://dx.doi.org/10.1049/el:19850192>.
- Olhoeft, G. R. (1976). Electrical properties of rocks. In R. G. Strens (Ed.), *The Physics and Chemistry of Minerals and Rocks* (pp. 262-278). London, U.K.: John Wiley Interscience.
- Pruess, K. A. (2004). A composite medium approximation for unsaturated flow in layered sediments. *J. Contam. Hydrol.*, 70(3-4), 225-247. <http://dx.doi.org/10.1016/j.jconhyd.2003.09.007>.
- Reynolds, J. A. (1957). Formulae for dielectric constant of mixtures. *Proc. Physical Soc., Section B*, 70(8), 769-775. <http://dx.doi.org/10.1088/0370-1301/70/8/306>.
- Robinson, D. A. (2004). Measurement of the solid dielectric permittivity of clay minerals and granular samples using a time domain reflectometry immersion method. *Vadose Zone J.*, 3(2), 705-713. <http://dx.doi.org/10.2113/3.2.705>.
- Robinson, D. A., & Friedman, S. P. (2003). A method for measuring the solid particle permittivity or electrical conductivity of rocks, sediments, and granular materials. *J. Geophys. Res.*, 108(B2), 2076. <http://dx.doi.org/10.1029/2001JB000691>.
- Roth, K., Schulin, R., Fluhler, H., & Attinger, W. (1990). Calibration of time domain reflectometry for water content measurement using a composite dielectric approach. *Water Resource Res.*, 26(10), 2267-2273.
- SAS. (2004). *SAS/STAT 9.1 User's Guide*. Cary, N.C.: SAS Institute, Inc.
- Simpkin, R. (2010). Derivation of Lichtenecker's logarithmic mixture formula from Maxwell's equations. *IEEE Trans. Microwave Theory Tech.*, 58(3), 545-550. <http://dx.doi.org/10.1109/TMTT.2010.2040406>.
- Stevens. (2007). Hydra Probe soil sensor. Portland, Ore.: Stevens Water Monitoring Systems, Inc. Retrieved from [www.stevenswater.com](http://www.stevenswater.com).
- Topp, G. C., Davis, J. L., & Annan, A. P. (1990). Electromagnetic determination of soil water content: Measurements in coaxial transmission lines. *Water Resource Res.*, 16(3), 574-582. <http://dx.doi.org/10.1029/WR016i003p00574>.
- Vaz, C. M., Jones, S., Meding, M., & Tuller, M. (2013). Evaluation of standard calibration functions for eight electromagnetic soil moisture sensors. *Vadose Zone J.*, 12(2), <http://dx.doi.org/10.2136/vzj2012.0160>.
- Webster, R. (2007). Analysis of variance, inference, multiple comparisons, and sampling effects in soil research. *European J. Soil Sci.*, 58(1), 74-82. <http://dx.doi.org/10.1111/j.1365-2389.2006.00801.x>.
- Wu, K. T., Yuan, Y. S., Zhang, R., Yan, X. Y., & Cui, Y. R. (2013). ZrTi<sub>2</sub>O<sub>6</sub> filled PTFE composite for microwave substrate applications. *J. Polymer Res.*, 20(8), 223-228. <http://dx.doi.org/10.1007/s10965-013-0223-4>.
- Yang, C. F., Wu, C. C., Su, C. C., & Chen, Y. C. (2009). The development of prediction method for the permittivity of epoxy/(Ba<sub>0.9</sub>Sr<sub>0.1</sub>)(Ti<sub>0.9</sub>Zr<sub>0.1</sub>)O<sub>3</sub> composites. *Appl. Physics A*, 97(2), 455-460. <http://dx.doi.org/10.1007/s00339-009-5241-z>.
- Zakri, T., Laurent, J. P., & Vauclin, M. (1998). Theoretical evidence for 'Lichtenecker's mixture formulae' based on the effective medium theory. *J. Physics D*, 31(13), 1589-159. <http://dx.doi.org/10.1088/0022-3727/31/13/013>.
- Zheng, Y., Wang, S., Feng, J., Ouyang, Z., & Li, X. (2005). Measurements of the complex permittivity of dry rocks and minerals: Application of the polythene dilution method and Lichtenecker's mixing formulae. *Geophysical J. Intl.*, 163(3), 1195-1202. <http://dx.doi.org/10.1111/j.1365-246X.2005.02718.x>.
- Zimmerman, R. W. (1989). Thermal conductivity of fluid-saturated rocks. *J. Petroleum Sci. Eng.*, 3(3), 219-227. [http://dx.doi.org/10.1016/0920-4105\(89\)90019-3](http://dx.doi.org/10.1016/0920-4105(89)90019-3).